Int. J. Environ. Res., 9(3):795-804, Summer 2015
ISSN: 1735-6865

Experimental Assessment of Sediment Transport and bed Formation of Sandy Beaches by Tsunami Waves

Daghighi, N., Chegini, A.H.N.*, Daliri M., and Hedayati D.

Faculty of Engineering, Guilan University, Rasht-Iran

Received 9 Aug. 2014; Revised 22 Oct. 2014; Accepted 26 Oct. 2014

ABSTRACT: All experiments in this study were carried out in a flume which was located in the hydraulic laboratory of technical faculty in Guilan University. The wave flume was 12 m long, 0.5 m wide, 0.5 m high and equipped with a wave-producing system and ultrasonic sensors. The objectives of current experimental study are to investigate sediment transport, bed formation and sustainability of sandy beaches with different grain size under tsunami attack. Sediment transport, caused by tsunamis, brings about severe damages to human beings, structures, beach topography and environment. Due to the devastating, destructive and scouring effect of tsunami waves, assessing their operation is of great importance. Experimental studies can be significantly helpful to evaluate the process of transported sediment by a tsunami. Three traps were employed to examine sediment transport in different parts of the beach. The achieved results indicated that wave breaking point has significant effect on the beach profile deformation and sustainability. Furthermore, grains with varying sizes, in the same conditions behave differently. As a result, for finer grains wave backwash has more effects on the sediment transport, while for coarser grains the wave itself has a main role in sediment transport.

Key words: Bed formation, Sandy beach, Sediment transport, Tsunami waves

INTRODUCTION

Tsunamis are sea surface gravity waves generated by underwater earthquakes, volcanic eruptions, large-scale coastal landslides, meteorite collisions and underwater nuclear explosions. Major tsunamis with large flow depth, high flow velocity and long wave period can erode, suspend and transport a large volume of sediment over a broad region. Sediment transport, caused by tsunamis, brings about severe damages to human beings, structures, beach topography and environmental process. Scour and erosion resulting from tsunamis can cause serious damages to the foundation of buildings, roads, highways, underground pipelines, coastal embankments or other shoreline structures. Due to their long periods, tsunamis are often modeled as solitary waves in physical and theoretical studies. In comparison to many other researches conducted in the field of morphological changes under wind waves and currents, few experimental studies were accomplished in association with erosion and sedimentation patterns caused by a tsunami. Kobayashi and Lawrence (2004) did laboratory experiments to examine the cross-shore sediment transport processes under breaking solitary waves on a fine sand beach. The initial beach slope of 1/12 was exposed to a positive solitary wave eight times. The beach was also rebuilt and exposed to a negative solitary wave eight times. Moronkeji (2007) has conducted physical experiments on the run-up and draw-down of solitary and cnoidal waves over a movable bed at two different beach slopes. Solitary wave heights of 10 cm, 30 cm, 50 cm, 60 cm and cnoidal waves of 30 cm as well as50 cm with wave length of12 m and8 m respectively were tested. Tsujimoto et al.(2008) examined the beach profile changes under solitary waves alone and in combination with regular waves. Young et al.(2010) investigated the erosion and deposition patterns under breaking positive solitary waves. Also they found that tsunami run-up and drawdown can cause liquefaction failure of coastal fine sand slopes due to the generation of high excess pore pressure. In other hand tsunami-induced sediment transport has been studied by several authors using various numerical models such as Simpson and Castelltort (2006), Goto and Imamura (2007) and Xiao et al. (2010). Although many researches have been conducted in relation to sediment transport, various mechanisms of this

*Corresponding author E-mail: chegini@guilan.ac.ir

process are still unknown which can be rooted in the complex hydrodynamic conditions of waves and geology.

MATERIALS & METHODS

Tsunamis called as "long waves" and/or "shallow-water waves" due to their long wave lengths, even if they occur in deep waters. Classic equations used for non-linear shallow water waves can be defined in the following manner in the direction of x:

$$\frac{\partial \eta}{\partial t} + \frac{\partial [(h+\eta)u]}{\partial x} = 0 \quad (1)$$

$$\frac{\partial u}{\partial t} + u\frac{\partial u}{\partial x} + g\frac{\partial \eta}{\partial x} = 0 \quad (2)$$

Where h stands for water depth, η for wave amplitude, u for the depth averaged velocity, t for time, and g for gravity acceleration. Carrier and Greenspan (1958), and Synolakis (1987) proposed different analytical solutions for those equations. Finally, the following equations were suggested for evaluating the water surface:

$$\eta = H \sec h^2 \sqrt{\frac{3H}{4h^3}}(x - ct) \quad (3)$$

$$c = \sqrt{g(H+h)} \quad (4)$$

$$u = \eta\sqrt{\frac{g}{h}} \quad (5)$$

Where H and h refer to wave height and water depth respectively, and c refers to wave celerity.

All experiments were done in a glass-side wall wave flume located in the hydraulics laboratory of technical faculty in Guilan University. The wave flume was 12 m long, 0.5 m wide and 0.5 m high. A gate was applied at upstream end of the flume in order to produce the waves, in a way that the water depth of upstream was more than downstream and the gate was suddenly opened to simulate conditions of tsunami waves. The produced wave was a solitary wave which is one of the most appropriate waves which can be simulated to tsunami waves. Three ultrasonic wave gauges were used to measure wave surface elevations and a 6-canal data logger, in which three sensors were active, was responsible for receiving the signals. Fig. 1 shows a photo of the flume with the wave-producing system and measurement tools.

The bottom of the flume was filled by sand with approximate thickness of 2 cm and finally beach was made with 1:14 slope. Two types of Caspian Sea sands with different mean diameters of 0.2, 0.8 and 2 mm and specific gravity from 2.6 to 2.7 gr/cm^3 were applied separately. Due to the produced shear stress and turbulences in the bed, the wave motion in the flume and its subsequent breaking cause sediment transport, that can be measured in different parts of the beach through the application of the traps. As a matter of fact, these traps were utilized to capture sediment transport while a wave was rushing up or down. Three traps, 48 cm long, 15 cm wide and 2 to 3 cm deep (on the basis of the coating thickness of the beach) were set on the beach region to collect the transported sediment. The first trap was set at the toe of the beach, while two other ones were set at distances of 120 and 240 cm from the toe. Various cameras were applied in different parts of flume to capture the wave breaking points and their operations on the beach. Fig. 2 shows an image of the sandy beach with its traps.

Tremendous discharge of tsunami waves energy in beach region cause sediment transport and significant deformation of coast sustainability. Due to the fact that most tsunami waves break before they reach the shore, so it was decided to investigate sediment transport and beach profile changes caused by broken solitary waves. Depending on the water height difference on two sides of gate, broken and unbroken waves and also bore can be produced. Various experiments were conducted with different water heights to choose the waves which were similar to real tsunami waves in terms of the height and speed, and were broken on the appropriate point. In other words, selected wave should not break before reaching the beach region, so that the impacts of wave on the shoreline could be seen. Finally, the waves with the same hydrodynamic conditions and different breaking points were selected. To determine the deformation of seabed and coast sustainability, two different materials (sands) with mean diameter of 0.8 and 2 mm were separately utilized in each test. For better observation of profile changes, eight successive tests were (at suitable intervals) accomplished for each grain size. A mechanical point gauge was employed to measure bed changes after the second, fifth and eighth tests. These tests were done at the different upstream and downstream water depths for each sand size. Upstream and downstream water levels of each test were used to name them, for instance, (UD29-14) shows that upstream level of the gate is 29 cm and its downstream level is 14 cm. When the heights of both sides reach the desired level, they are

Fig. 1. A view of the flume, measurement tools, and wave-producing system

Fig. 2. Sandy beach and its traps

recorded by software which controls the sensors. Through rotating the handle of the wave making gate, a wave will flow toward the flume, while wave detectors record the water levels. In order to describe the beach region and location of measurement tools, Cartesian coordinate system is designed in a way that X axis is toward the shoreline and Z axis is upward. Sensor 1 is located at a distance of 0.5 m from the toe of the beach to recognize the incoming wave before reaching the beach region, and two other sensors are respectively set at distances of 0.7 m and 1.7 m from the toe to examine the changes of water surface due to wave shoaling and wave breaking. The obtained results from the sensors indicated that the incoming waves heights was about 10.5 cm and the waves were respectively broken at distances of 120 cm and 170 cm from the toe of the beach. Table 1 shows the waves characteristics for each test. Fig. 3 demonstrates a view of the flume and the sensors location (which are shown by letter S).

RESULTS & DISCUSSION

In this section, deformation of beach profile under tsunami waves for the sands particles with mean diameter of 0.8 mm and 2 mm was investigated. Fig. 4 indicates temporal changes of solitary wave profile generated by wave making gate for experiment UD29-14.

Grilli et al. (1997) defined the dimensionless slope parameter S_0 for solitary waves as a breaking criterion as follows:

$$S_0 = 1.521\frac{s}{\sqrt{H/h}} \quad (6)$$

Table 1. Characteristic of generated waves in order for assessment of beach profile deformation

Test	Upstream depth (cm)	Downstream depth (cm)	Breaking point distance from the toe (cm)	Number of tests on each particle	Wave breaking type
UD29-14	29	14	120	8	Plunging
UD32-17	32	17	170	8	Plunging

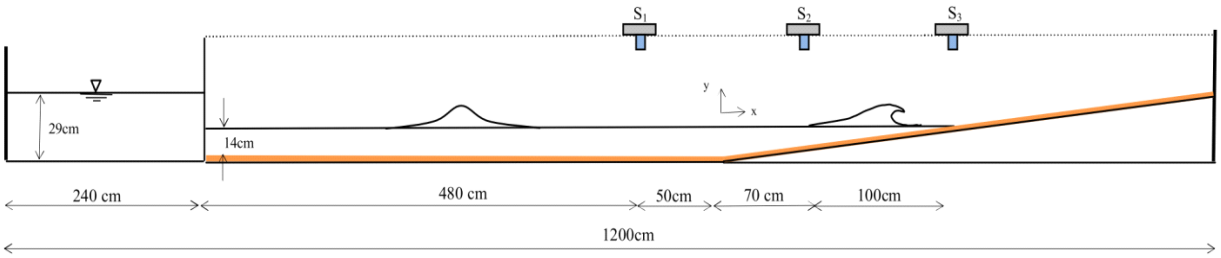

Fig.3. Experimental setup used for assessment of beach profile deformation (UD29-14)

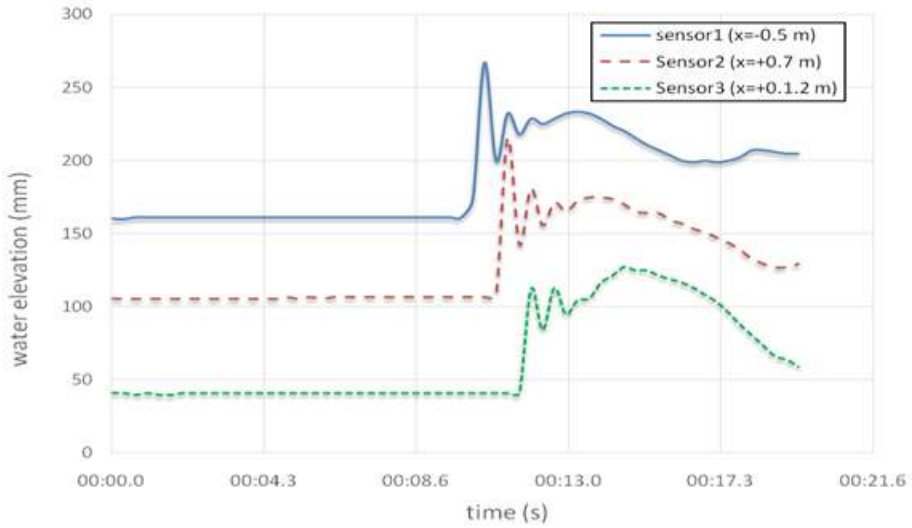

Fig. 4.Temporal changes profile of solitary wave (UD29-14)

Where s represents seabed slope, H and h represent wave height and water depth respectively.

With using dimensionless slope parameter, it can be predicted whether a solitary wave will break or not and which type of wave breaking will occur. Conducted experiments showed that waves with dimensionless slope parameter $S_0 < 0.37$ are broken waves, and if $0.025 < S_0 < 0.3$ wave breaking type is plunging break. These results were confirmed through numerical and experimental approaches. All generated waves in this study were breaking wave and kind of plunging. In order to assess the wave velocity, the distance was divided by the time between sensors 1 and 2 and the result was $1.71\, m/s$. The velocity of a solitary wave, based on equation 4, was calculated about $1.55\, m/s$, which is consistent with the experimental results. In both experiments (UD29-14and UD32-17), the waves were broken before reaching the shoreline on a thin layer of water. Observing the recorded videos, it can be seen that sediment concentration does not enhance suddenly after the wave breaking and no considerable turbulence occurs in that moment. It can be resulted from the thin layer of water on which the wave breaks. And then, a bore is constructed which separates a large volume of sands from the bed and moves forward due to the water momentum. At the highest level of the wave run up, water depth is considerably low, sediment concentration is high, and flow velocity is about zero, all these conditions cause sediment deposition in the bed. After the maximum run up the flow retreats seaward, this process is consisting of an intensive sheet flow, hydraulic jump, and a recirculation region of the flow. In this region, water

depth is low, while the backward flow velocity and sediment concentration are high which lead to net erosion in the bed. While wave is running-down, it faces a large amount of water and a hydraulic jump occurs. When water with high concentration, enters recirculation flow of hydraulic jump, the flow velocity decreases suddenly and sediments started to deposit in that region. At last, a net deposition happens around the wave breaking point. During the process of carrying out experiments and observing waves breaking and their operation on the beach, many cameras were set in different parts of the beach to record the events. Figs 5 and 6 respectively indicate the wave breaking moment and hydraulic jump in backward flow.

The initial beach slope was about 1:14, it was the result of many waves with smaller amplitudes which have flown to saturate the bed. Then, the beach profile was measured by mechanical gauge and it was considered as the initial bed. Figs 7 to 10 show the bed profile changes with mean sand diameter of 0.8 and 2 mm under waves UD32-17 and UD29-14.

Comparing figs 7 to 10 proves the importance of breaking point in bed morphological changes. Further distance of breaking point from the beach toe leads to further deposition and erosion regions. As it can be noticed in experiment UD29-14with the breaking point of 120 cm from the beach toe (figs 7 & 9), erosion highly decreases from the distance of 220 cm towards the toe. Moreover, deposition region occurs near the breaking point. In experiment UD32-17 with the breaking point of 170 cm from the toe (figs 8 & 10), erosion continues even to the distance of 300 cm. Considering figs 7 to 10, it can be concluded that the most erosion of beach region occurs over the sea water level (towards the shoreline), while the deposition occurs under the sea water level (around the breaking point). It is observed that by repeating the experiments a convergence between the achieved profiles and previous tests' profiles can be observed. It can be also noticed that the erosion area is wider than deposition area, while the latter is more in depth. It is due to the fact that the erosion emerges from the breaking point to the wave run up level, but deposition happens after the hydraulic jump at the breaking point, so the deposition region is strongly dependent on the turbulent area of hydraulic jump.

Fig. 5. Wave breaking moment

Fig. 6. Hydraulic jump

This section deals with the amount of transported sediment that wave causes at different points or moments. Three traps were used to measure the amount of sediment transport. Trap 1 was installed at the beach toe; traps 2 and 3 were set at distances of 120 cm and 240 cm from the first one. These traps were utilized to assess the amount of sediment transport caused by 5 solitary waves in various heights. Sands with three different mean diameters of 0.2, 0.8 and 2 mm were separately applied to examine sediment transport for each experiment. Related data for each wave is shown in Table 2. Fig. 11 illustrates the flume, sensors, traps and cameras in most tests. In this figure, T stands for trap, S stands for ultrasonic sensor and C stands for camera.

As it has been mentioned, incident waves are considerably effective in sediment transport while rushing up and rushing down the beach. In the current study, all waves broke between traps 2 and 3 and the height of incident waves was calculated about 10 to 11 cm. When a wave is moving forward, some sediment are transported to the traps before rushing down which are called 'forward sediments'. When the wave reaches the highest level, it starts retreating and transports a huge amount of sediments to the traps; these sediments are called 'backward sediments'. Three cameras record all these processes at the top of the traps. Having completed each experiment, water inside the flume drains, sediments are collected from the traps and weighed after drying. Owing to the fact

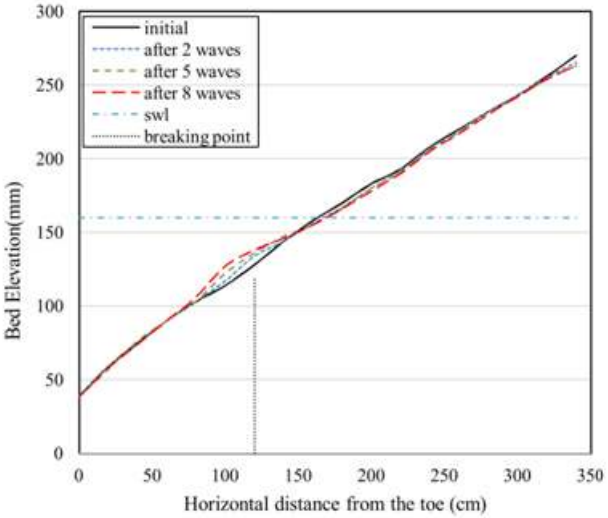

Fig. 7. Beach profile changes (d_{50}= 0.8 mm) – wave condition UD29-14

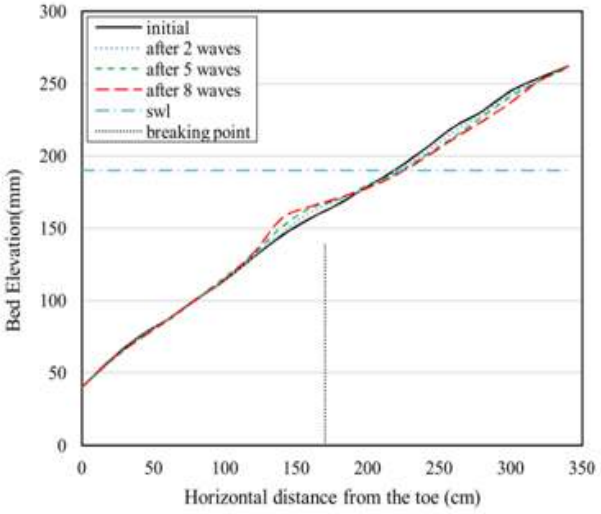

Fig. 8. Beach profile changes (d_{50}= 0.8 mm) - wave condition UD32-17

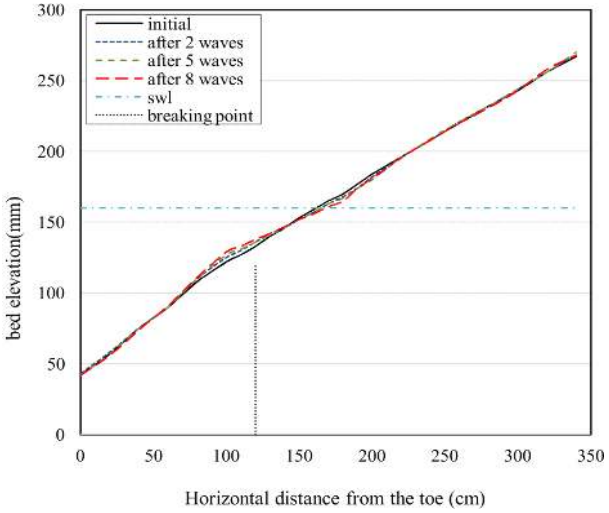

Fig. 9. Beach profile changes (d_{50}= 2 mm) -wave condition UD29-14

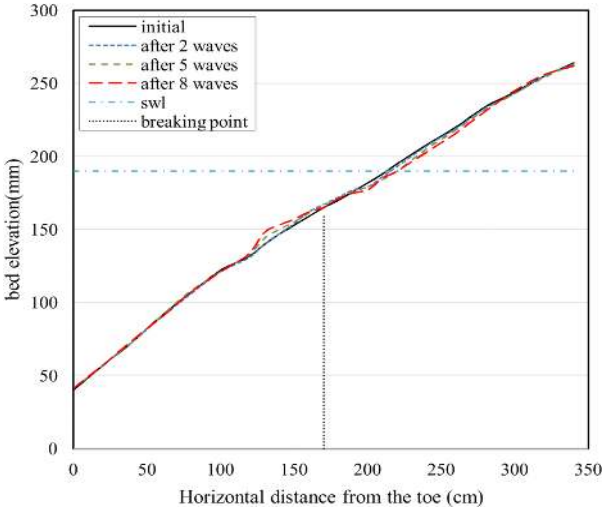

Fig. 10. Beach profile changes (d_{50}= 2 mm) - wave condition UD32-17

Table 2. Characteristics of generated waves in order to measure sediment transport

Test number	Upstream depth *(cm)*	Downstream depth *(cm)*	Breaking point distance from the toe *(cm)*	Wave breaking type
1	29	14	120	Plunging
2	30	15	135	Plunging
3	31	16	150	Plunging
4	32	17	170	Plunging
5	33	18	190	Plunging

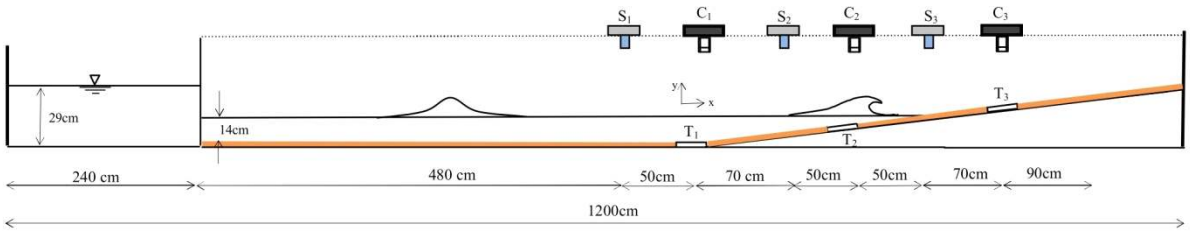

Fig. 11. Illustration of experimental setup used for assessment of sediment transport

that intervals between rising and lowering levels of the incident wave of each experiment were too short and there was not enough time to collect and weigh the forward sediments, recorded videos were applied to estimate forward sediments weights and subtracting forward sediments from the total sediments equal backward sediments in each trap.

The objective of this part of the study was to examine the parameter of transported sediment volume in width for each wave. Parameter of transported sediment volume (V_S) is dependent upon many factors such as wave height (H), water depth (h), beach slope (s), sand diameter (D), Water density (γ_w), Sand density (γ_s), distance from the beach toe to the breaking point (X_b) and gravity acceleration (g). Since the assessment of all aforementioned factors is not possible in an article, dimensional analysis approach has been applied. Buckingham π theorem was used for computing sets of dimensionless parameters from the given variables:

$$f(V_S, H, h, s, D, \gamma_w, \gamma_s, X_b, g) = 0 \quad (7)$$

(8)

$$\pi_1 = \frac{V_S}{H^2},\ \pi_2 = \frac{X_b}{H},\ \pi_3 = \frac{h}{H},\ \pi_4 = \frac{D}{H},\ \pi_5 = \cot s,\ \pi_6 = \frac{\gamma_s}{\gamma_w} = G_s$$

Where G_s represents speciûc gravity of sand. Dimensionless parameter of transported sediment volume (π_1) can be considered as a function of five other dimensionless parameters:

$$\frac{V_S}{H^2} = F\left(\frac{DG_s X_b}{hH}\cot s\right) \quad (9)$$

In order to obtain F function, (V_S/H^2) should be calculated using laboratory data and based on dimensionless parameter of $(DG_s X_b \cot s/hH)$; a logical relationship should also be established between them. Dimensionless parameter of $(DG_s X_b \cot s/hH)$ is referred as Parameter λ is directly associated with Wave breaking point (X_b), while it is in reverse to water depth (h). Due to the fact that water depth changes are not much in comparison to waves breaking points changes, it can be concluded that parameter λ increases with increasing wave breaking point. Notice that other factors of parameter λ are approximately fixed in this experiment. Experimental observations indicated that none of the waves could transport significant amount of sediment to the trap 1. Due to the fact that trap 1 was set at the beach toe, all waves were broken after passing this trap, so no discharge of energy and sediment transport happened in that area. Furthermore, the incoming waves at this point are in deeper water in proportion to the breaking area. Subsequently, waves are less effective on the bed in this region and they will not be capable of moving much sand.

Figs 12 to 14 show changes of dimensionless parameter of transported sediment volume in width (V_S/H^2) with respect tothe parameter λ for the sands with mean diameter of 0.2, 0.8 and 2 mm in trap 2. As it can be seen in fig. 12, backward sediments are significantly more than forward sediments in trap 2. Since almost all waves break after trap 2, and due to the fact that downstream water level increases about 1 centimetre in each step of the experiment, increasing the amount of parameter λ cannot significantly change forward sediment, but it decreases backward sediment. It can be the result of increasing the distance between hydraulic jumps and trap 2 when drawing back. As it was mentioned in the section of bed morphological results, water flow experiences a hydraulic jump near breaking point when retreating, and this highly decreases the velocity of the sheet flow and leads to deposition at this point.

So, the waves which break with more distance from trap 2, deposit sediment sat the further distance (due to the hydraulic jump occurrence in further region), and so that amount of sediment trapped in trap 2 will be decreased . Finally it can be said that the increase of parameter λ can decrease backward sediment in trap 2.

Fig. 13 shows changes of the parameter (V_S/H^2) with respect to the parameter λ in trap 2 for the sand withd_{50}= 0.8 mm. Similar to fig. 12, this figure indicates that increasing the amount of the parameter λ cannot significantly change forward sediment, but it has slightly reduced. Longer distance of breaking point (X_b) from trap 2 and the increase of the parameter λ can cause a hydraulic jump at further distance from the trap, and as a result, less sand will be captured in trap 2. As it can be noticed in experiment 1 (UD29-16), since the wave was broken on trap 2 (X_b =115 cm), the most amount of sediment was captured in trap 2 as backward sediment. The significant role of breaking point in transporting sediment of beach region can be clearly seen in this figure. In fact, although breaking points of experiments 1 and 5 are about 70 cm apart, the amount of sediment transport has decreased more than %97 in these two experiments. Regarding forward sediments and backward sediments in fig. 13, this conclusion can be drawn that backward flow has more effect on sediment transport in proportion to forward flow (incident wave) in trap 2. Also it is obvious that the totalsediment transport ofthe waves which break far from trap 2 (increasing the amount of the parameter λ)becomes lower.

Fig. 14 shows changes of the parameter (V_S/H^2) against the parameter λ in trap 2 for the sand with d_{50}= 2 mm. Characteristics of this figure is

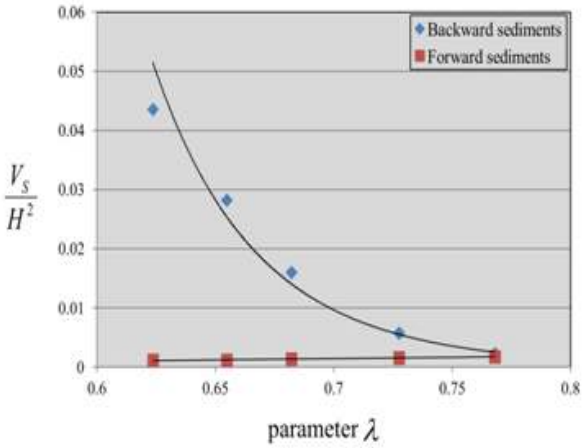

Fig. 12.Variation of (V_S/H^2) against parameter λ for trap 2 (d_{50}= 0.2 mm)

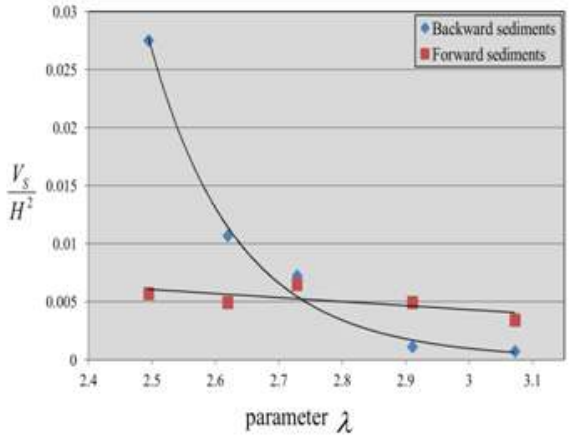

Fig. 13.Variation of (V_S/H^2) against the parameter λ for trap 2 (d_{50}= 0.8 mm)

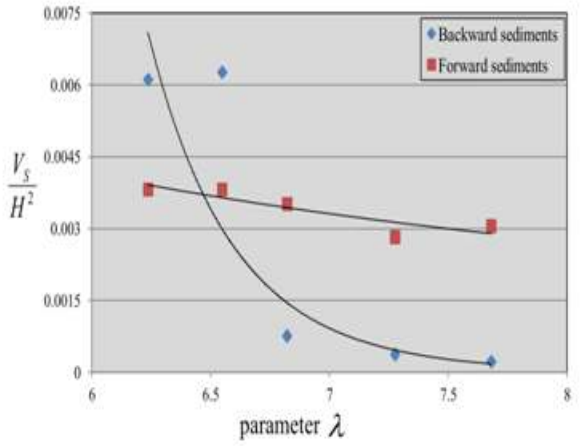

Fig. 14.Variation of (V_S/H^2) against the parameter λ for trap 2 (d_{50}= 2 mm)

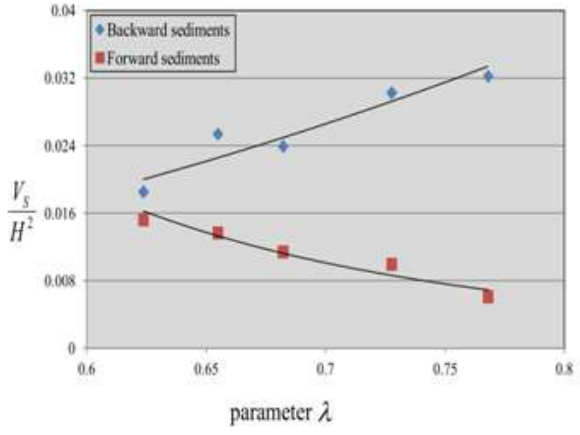

Fig. 15.Variation of (V_S/H^2) against the parameter λ for trap 3 (d_{50}= 0.2 mm)

similar to figs 12 and 13. Based on aforementioned figs (12, 13), it can be concluded that total sediment transported to trap 2 for d_{50}= 0.2 mm results from the backward flow, and the backward sediments is more than forward sediments for various amounts of the parameter λ (fig. 12). Increasing the size of sands can decrease backward sediments in trap 2. For sands with mean diameter of 0.8 mm and 2 mm, especially for the latter one, from the third experiment ahead (where breaking point and trap 2 are about 30 cm apart), forward sediments is more than backward sediments. It means that the effect of backward flow will greatly reduce when distancing the breaking point from trap 2. As a matter of fact, enhancing the size and weight of the sands leads to a decrease in backward sediments.

Fig. 15 shows changes of parameter (V_S/H^2) against the parameter λ for the sands with d_{50}=0.2 mm in trap 3. All the waves broke before reaching trap 3. Increasing the amount of the parameter λ leads to decrease forward sediment in trap 3. In fact, it can be stated that the further a breaking point is from trap 3, the more opportunity it has to flow on the bed, so that it can suspend more sediments and transport them to trap 3. Experiment 5 which has the nearest breaking point to trap 3 (40 cm) cannot transport many sediments to trap 3. Fig. 15 also indicates an increase in backward sediment in trap. The further a wave breaks before reaching trap 3, the deposition will occur at a longer distance during drawing back with a hydraulic jump. Therefore, the waves which break nearer to trap 3, more sediment will be transported to the trap during retreating. Fig. 15 indicates that backward sediment is always more than forward sediment, even in the places after wave breaks (trap 3), for sand with d_{50}= 0.2 mm.

Figs 16 and 17 show changes of parameter (V_S/H^2) against the parameter λ for the sands with mean diameter of 0.8 mm and 2 mm in trap 3. Like sand particle of 0.2 mm, increasing the parameter λ leads to decrease forward sediment, and increase backward sediment. It can be noticed that in reverse with the fig. 15, for all amounts of parameter λ forward sediment is more than backward sediment. In fact, the capability of backward flow in transporting the sands to trap 3, which is located after the breaking point, considerably decreases. The results indicate that the capability of backward flow in sands transport (0.8, 2 mm) to trap 3, which is located after the breaking point, considerably decreases. It happens because sediment will rapidly deposit due to relative heaviness of particles. Thus, in backward flow sediment concentration decreases and a few sediments were transported to further distances. As it can be observed in fig. 17, this process is more clear for sands with d_{50}= 2 mm. Considering the shown figures, the significant role of breaking point and sand size in the volume of transported sediment can be noticed when the slope is determined and incoming waves have the same characteristics and conditions.

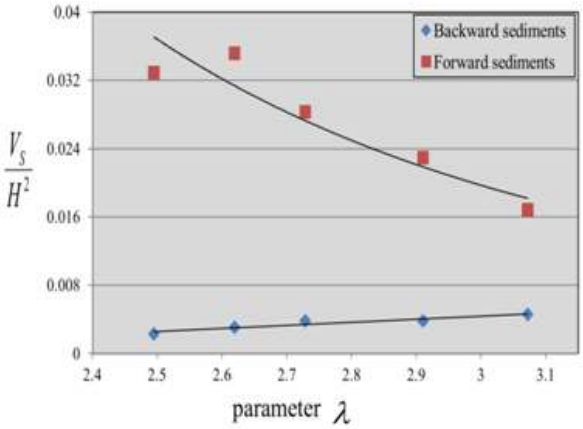

Fig. 16.Variation of (V_S/H^2) against the parameter λ for trap 3 (d_{50}= 0.8 mm)

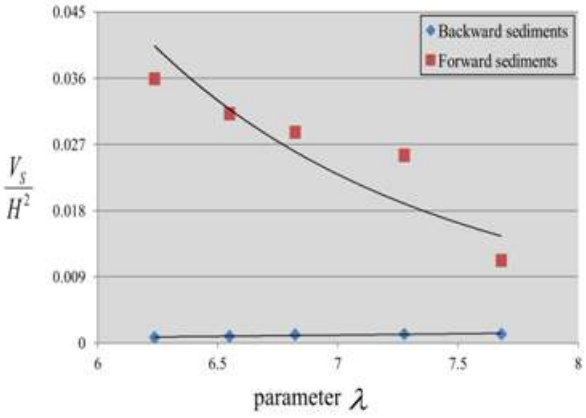

Fig. 17. Variation of (V_S/H^2) against the parameter λ for trap 3 (d_{50}= 2 mm)

CONCLUSIONS

The current study was an experimental one which was conducted in the flume of Gilan University and aimed to investigate sediment transport, bed deformation and sustainability of sandy beaches caused by tsunami waves. Two series of experiments were separately carried out to assess the changes of beach profile for the grains with mean diameter of 0.8 and 2 mm. Solitary waves were produced in each experiment at the depths of 14 and 17 cm, and 8 solitary waves with the approximate height of 10.5 cm were successively (at appropriate intervals)

generated at each depth. A mechanical point gauge was employed to measure bed changes after the second, fifth and eighth tests.

It was observed that when a wave breaks, it causes a suspension of sediments which transport them forward while rushing up. Moreover, when the flow drawing down, sediments will be moved by the flow and at last after a hydraulic jump, the deposition will occur near the breaking point. The achieved findings indicated that in solitary waves with the same height, when water depth increases, the breaking point will be located further from the beach toe. Longer distance of breaking point from the beach toe caused further deposition and erosion which shows a significant role of breaking point in beach actions. Furthermore, the results demonstrated that the most erosion of beach regions occurs over the sea water level (towards the shoreline), while deposition occurs under the sea water level (around the breaking point). In order to assess transported sediment caused by tsunami waves, three separate experiments were conducted on the sands with different mean diameter of 0.2, 0.8 and 2 mm, thus three traps were employed to examine sediment transport in different parts of the beach. Related data for each wave was shown in Table 2. The findings indicated that tsunami waves cannot transport much sediment in regions far from the beach due to much depth of the water (like trap 1 in this experiment); while in beach regions, they are greatly destructive and capable of transporting a large amount of sediments. All the waves in this experiment were broken between traps 2 and 3 (shown in fig.11). Results shows that the regions before breaking points (like trap 2), for sands of 0.2 mm., increasing distance from the trap cannot bring about considerable changes in the amount of forward sediment, while for sands of 0.8 and 2 mm this amount has decreased. In backward flow, for all three types of the sands, increasing the distance from the trap decreased the amount of transported sediment to the trap.

The findings demonstrated that for sands of 0.2 mm, almost all transported sediments to the trap are resulted from the backward flow, while for the sands of 0.8 and 2 mm, with furthering the breaking point from the trap, backward sediment would be less than forward sediment. In fact, relative heaviness of the sands caused rapid deposition in a way that the capability of backward flow decreases in moving the sediments. The experiments also showed that regions after the breaking point (such as trap 3 in fig. 11) for all three types of the sands, shorter distance of breaking point from the trap caused a decrease in the volume of forward sediment. While in backward flow, through decreasing the distance of breaking point from the trap, backward sediment increased for sands of 0.2 and 0.8 mm and no specific change was observed for sands of 2 mm.

In all experiments for sands of 0.2 mm backward sediment was more than forward sediment. It means that backward flow, as mentioned for regions before wave breaking points, had a great effect on sediment transport after breaking point. Sands of 0.8 and 2 mm, a completely different event occurred, in a way that forward sediment were much more than backward sediment, especially for sands of 2 mm. Therefore, this conclusion can be drawn that in addition to breaking point, sand size is of great importance in the amount of transported sediment. Also it can be mentioned that backward flow is more dominant for finer sands (0.2 mm), while forward flow wave itself is dominant for coarser sands (0.8 , 2 mm).

REFERENCES

Carrier, G. and Greenspan, H. (1958). Water waves of finite amplitude on a sloping beach. Journal of Fluid Mechanics, **4(1),** 97-109.

Goto, K. and Imamura, F. (2007). Numerical models for sediment transport by tsunamis. The Quaternary Research, **46 (6),** 463–475.

Grilli, S. T., Svendsen, I. A. and Subramanya, R. (1997). Breaking criterion and characteristics for solitary waves on slopes, Journal of Water, Port, Coastal Ocean Engineering, **123(3),** 102-112.

Kobayashi, N. and Lawrence, A.)2004). Cross shore sediment transport under breaking solitary waves. Journal of Geophysical Research., **109,** C030047.

Moronkeji, A. (2007, August). Physical modelling of tsunami induced sediment transport and scour. (Paper presented at the 2007 Earthquake Engineering Symposium for Young researchers. Seattle, Washington).

Simpson, G. and Castelltort, S. (2006). Coupled model of surface water flow, sediment transport and morphological evolution.Computers and Geosciences, **32(10),** 1600–1614.

Synolakis, C. E. (1987). The run-up of solitary waves, Journal of Fluid Mechanics, **185,** 523–545.

Tsujimoto, G., Yamada, F. and Kakinoki, T. (2008). Time-space variation and spectral evolution of sandy beach profiles under tsunami and regular waves. (Paper presented at the International, Offshore and Polar Engineering Conference, Vancouver, Canada).

Young, Y. L., Xiao, H. and Maddux, T. (2010). Hydro-and morpho-dynamic modeling of breaking solitary waves over a fine sand beach. Part I: Experimental study. Marine Geology, **269(3),** 107-118.

Xiao, H., Young, Y. L. and Prevost, J. H.(2010). Hydro- and morpho-dynamic modeling of breaking solitary waves over a fine sand beach. Part II: Numerical simulation, Marine Geology, **269(3-4),** 119-131.